The International Journal of Advanced Manufacturing Technology (2019) 100:1463–1473
https://doi.org/10.1007/s00170-018-2783-2

ORIGINAL ARTICLE

Friction stir vibration processing: a new method to improve the microstructure and mechanical properties of Al5052/SiC surface nanocomposite layer

M. Abbasi[1] · M. Givi[1] · A. Ramazani[2]

Received: 2 July 2018 / Accepted: 25 September 2018 / Published online: 4 October 2018

Abstract
Friction stir processing (FSP) is a surface processing method to modify the microstructure and enhance the mechanical properties of metal surface. This process is also numerated as a method to incorporate second-phase nanoparticles into microstructure and form surface composites. In the current research, the work specimen is vibrated normal to processing line during FSP. Transverse and rotation movements of shoulder are accompanied with vibration motion of specimen. This new process is entitled FSVP (friction stir vibration processing). The effect of FSP and FSVP processes on microstructure and mechanical properties of Al5052 alloy matrix composite incorporated SiC nanoparticles is analyzed. The results show that the presence of vibration during FSP leads to the grain size decrease in the stir zone and it enhances the homogeneity of particle distribution. The results indicate that strength and ductility of friction stir (FS) processed specimens are lower than those processed by FSVP. These are related to increased deformation and strain of soft material in the stir zone as vibration is applied which promotes the dynamic recovery and recrystallization during FSP. The results also imply that the microstructure is refined more and the strength and the hardness of friction stir vibration (FSV) processed specimens increase as vibration frequency enhances.

Keywords Friction stir vibration processing · SiC nanoparticles · Surface composite · Microstructure · Mechanical properties

1 Introduction

FSP is a thermo-mechanical process which induces a specific thermal cycle in the processed zone of metal surface. The rotating tool penetrates into the workpiece until the shoulder contacts the upper surface of workpiece and is then traversed along the surface at a controlled velocity and rotation speed. The heat generated by friction and deformation leads to a soft material around the tool that flows from the front to the back of the tool and around the pin. FSP leads to grain refinement, dissolution of strengthening phases, and removal of cast porosities in case it is applied for surface modification of cast substrates [1]. The equiaxed dynamically recrystallized grains with large fraction of high angle grain boundaries are the microstructural characteristics of a FS processed zone [2, 3].

FSP also changes the size, type, and distribution of the strengthening particles in the microstructure. Arora et al. [4] found that Al_2Cu strengthening particles within the matrix of the 2xxx series aluminum alloys were dissolved into the stir zone due to the heat generated during the FSP. Fu et al. [5] concluded that these strengthening particles were dissolved during the FSP method and after cooling, the particles were re-precipitated into the microstructure.

Hannard et al. [6] found that FSP increased the fracture strain of the Al alloy 6056 and made the microstructure more isotropic. Their micro-tomography results showed that FSP affected the main causes of ductility loss in metallic alloys. It broke the large intermetallic particles into smaller and thus stronger ones, closed the pre-existing porosities, and randomized the iron-rich intermetallic particle distribution. Large particles break easily during deformation and the increase of FSP passes enhances the proportion of particles with an aspect ratio close to one. Leal et al. [7] applied FSP to promote the microstructure and electrical conductivity of the copper alloy C12200. They studied the effect of tool rotation and traverse

✉ A. Ramazani
ramazani@umich.edu

[1] Faculty of Engineering, University of Kashan, Ravandi Blvd., Kashan, Iran

[2] Department of Aerospace Engineering, University of Michigan-Ann Arbor, Ann Arbor, USA

speeds as well as tool geometry on characteristics of processed alloy. They found that tool geometry had a strong effect on microstructure and different properties of FS processed specimens. They also concluded that electrical conductivity of the FS processed copper governed by the density of dislocations inside the grains and the electrical conductivity of the processed material increased as dislocation density decreased.

Production of bulk ultrafine grained composites by incorporating reinforcing particles such as SiO_2, SiC, TiO_2, and NiTi in metallic plates such as aluminum, magnesium, and copper are some examples of application of FSP [8–12]. Ghanbari et al. [13] studied the effect of FSP pass number on microstructure and wear behavior of Al2024 matrix composite incorporated SiC nanoparticles and found that the particles distribution homogeneity within the stir zone increased as the number of passes increased. They also concluded that the hardness decreased and the wear resistance increased as the pass number increased.

Ghanbari et al. [14] also studied the effect of heat treatment on microstructure and wear resistance of Al2024 matrix composite incorporated SiC nanoparticles and found that solution annealing and artificial aging after FSP increased the hardness and improved the wear resistance. The hardness increase was related to the dissolution of the coarse S-phase precipitations during the solution annealing and re-precipitation of fine S-phase (Al_2CuMg) during artificial precipitation aging.

Shafiei et al. [15] produced composite of Al6082/Al2O3 by FSP and explained that the hardness increase in the produced composite was related to the decrease of grain size and the Orowan mechanism. Ahmadifard et al. [16] fabricated Al5083/SiC surface composite by FSP and evaluated the effect of FSP pass number on characteristics of FS processed specimens. Al5083 alloy sheet with thickness of 5 mm was used as base material and SiC micron-sized powders were applied as strengthening particles. They found that microhardness and ultimate tensile strength improved as pass number increased. They concluded that as pass number increased, the agglomeration of second-phase particles decreased.

Khodabakhashi et al. [17] employed the FSP to fabricate a surface composite layer. Graphene nanoplatelets (GNPs) were dispersed into an Al5052 aluminum alloy. They observed a fine equiaxed recrystallized grain structure with an average size of 2.1 μm in the stir zone (SZ). They also reported that hardness and yield strength increased by 53% and three times, respectively, compared to the base material.

Dadaei et al. [18] investigated the role of two reinforcing particles, SiC and Al_2O_3 nanoparticles, incorporated in surface composite developed on AZ91 magnesium alloy by FSP. They found that strength and hardness increased as reinforcing particles were added to matrix. They also concluded that SiC particles were more beneficial than Al_2O_3 particles.

In the current research, a new method is applied to modify the microstructure and enhance the mechanical properties of surface composite layer developed on Al5052 alloy by FSP. In this method, the workpiece is vibrated normal to processing line during FSP. This method is entitled friction stir vibration processing (FSVP). Microstructure and mechanical properties of FS and FSV processed specimens are compared.

2 Materials and methods

Al5052 aluminum alloy sheet with thickness of 3 mm was applied for experiments. The chemical composition of the studied sheet is presented in Table 1. The sheet was cut into specimens with dimension of 100 × 200 (mm × mm).

A V-shaped surface groove with 2-mm width and 1.5-mm depth was machined along the length and in the middle of the each specimen. The specimens were all cleaned by methanol to remove any oil and debris. The groove on each specimen was filled with SiC nanoparticles as second-phase and reinforcing particles. SiC nanoparticles with nominal diameter of 20 nm were utilized. The weight of powders used for each specimen was 0.06 g. The specimen, contained powders in groove, was fixed on fixture and fixture was installed on milling machine. In the first pass, the groove surface was rubbed by a pin-less FSP tool with just shoulder to cover the groove surface up and to encapsulate the particles within the groove. This inhibits the escape of particles during proceeding FSP or FSVP passes. FSP and FSVP were conducted by application of a milling machine. For FSP, the fixture was clamped on the milling machine, while for FSVP, the fixture was clamped on a vibrating machine installed on the milling machine. The vibrating machine changes the rotating movement of motor shaft to linear and reciprocatory movement of vibrating plate by a camshaft mechanism. Schematic design of machine used for FSVP as well as great detail of cam follower is presented in Fig. 1. Using turning process, a part of shaft is made acentric. As shaft rotates, the acentric part impacts the walls of channel and leads to motion of vibrating plate. Vibrating plate moves on two guide rails. Due to excessive wear between part and wall, the impact of part was transferred to the wall through a ball bearing. Based on design, the maximum displacement of vibrating plate is 0.5 mm. Vibration frequency was adjustable and it was controlled by a driver.

Two-piece FSP tool, consisted of shoulder from heat-treated M2 steel and pin from carbide tungsten, was applied for processing. Schematic design of shoulder and pin is presented in Fig. 2. Different rotation and transverse speeds values were tried to find the optimum values, based on trial

Table 1 Chemical composition of the studied aluminum alloy (wt%)

Al	Mg	Cr	Si	Cu	Mn	Zn	Fe	Other
Balance	2.5	0.3	0.25	0.1	0.1	0.1	0.35	0.15

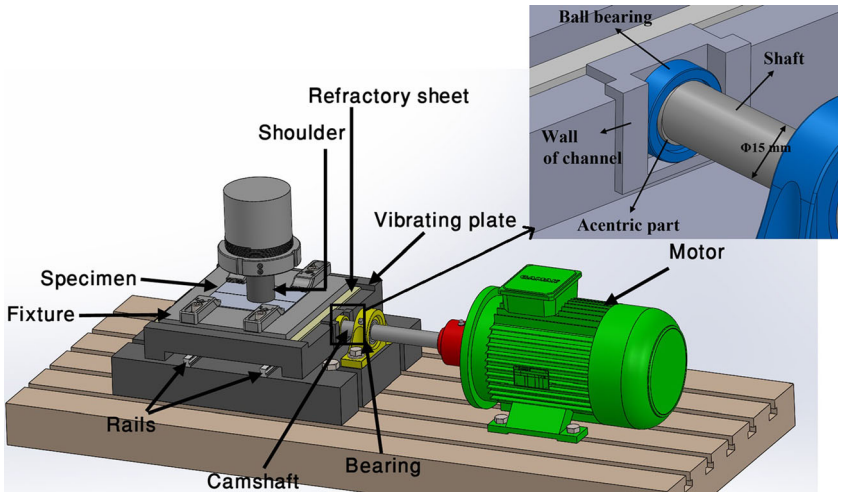

Fig. 1 Machine used for FSVP

and error method, for FSP. The findings showed that FSP with rotation speed of 1150 rpm and transverse speed of 31.5 mm/min resulted in surface with good appearance and fair mechanical properties. These optimum values of the rotation and transverse speeds were also applied for all FSVPs. Different vibration frequencies were applied, 20, 35, and 50 Hz. The tilt angle for all FSPs and FSVPs was considered to be 2°.

Microstructure was revealed by metallography techniques based on ASTM-E3 [19]. The etchant consisted of 4.2 g picric acid, 10 mL acetic acid, 10 mL water, and 70 mL ethanol was used for etching and it was applied for 5 s. Microstructure was analyzed utilizing light optical microscopy (LOM) and scanning electron microscopy (SEM). Uniaxial tensile test based on ASTM-E8 [20] was performed to obtain the stress-strain curves of processed specimens. Tensile test specimens, normal to processing direction, were prepared from FS and FSV processed specimens using electro discharge machining (wire cut) while the stir zone was located in the middle of gauge length. During the tensile tests, the crosshead speed was 0.5 mm/min. Three tensile tests were carried out for each processing condition. Vickers microhardness for different zones of FS and FSV processed specimens was measured based on ASTM-E92 [21]. Load was 100 gf and dwell time was 10 s. Five repeats were considered for each measurement. The distance between test points was higher than six times the diameter of indentations.

3 Results and discussion

3.1 The effect of vibration

Cross sections of FS and FSV processed specimens are shown in Fig. 3. Both specimens show a defect free stir zone. The processed zone size for FSV processed specimen is larger than that for the other one. This relates to vibration of workpiece during FSVP which results in a larger processed zone.

Microstructures of processed zones for FS and FSV processed specimens are observed in Fig. 4. The three areas, namely stir zone (SZ), thermo-mechanically affected zone (TMAZ), and heat affected zone (HAZ) which are formed during FSP, are observed in Fig. 4. The grains in the HAZ experience heat and do not deform while the grains within the TMAZ experience heat and slightly deform. The finest grains are observed in the stir zone which grains, in this zone, deform excessively during FSP and accordingly fine and co-axial grains are produced.

It is also observed in Fig. 4 that the stir zone grain size for the FSV processed specimen is lower than that for the FS

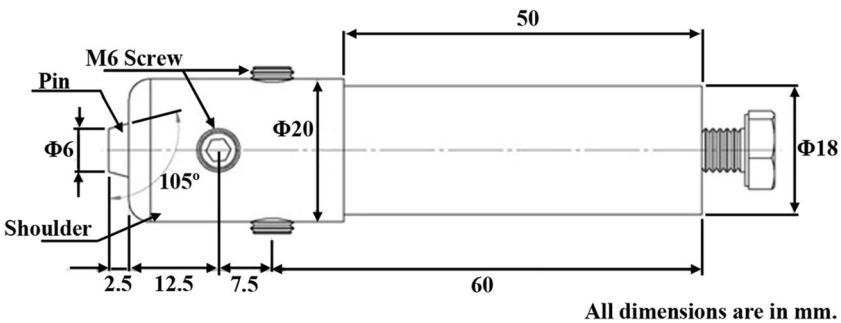

Fig. 2 Schematic design of tool used for FSP and FSVP

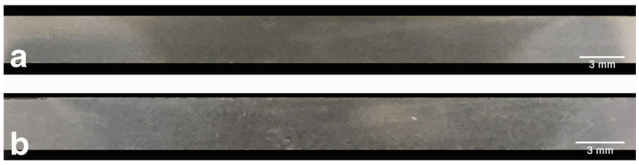

Fig. 3 Cross section macrostructure of processed specimens: **a** FS and **b** FSV processed specimens

processed specimen. It is known that grain size decreases during FSP due to dynamic recrystallization [22, 23]. In fact, FSP is a thermo-mechanical process which deforms the soft material in the stir zone severely [23]. This phenomenon produces vast amount of dislocations which can reorient themselves during dynamic recovery and form low-angle grain boundaries within parent grains. As deformation proceeds, dynamic recrystallization occurs and low-angle grain boundaries within grains transform to high-angle grain boundaries and consequently low-size grains are constituted in the microstructure [24, 25]. During FSVP, the workpiece vibration is accompanied with tool transverse and rotation movements. Consequently, more deformation and strain is applied on the material in the stir zone. Based on findings [26, 27], dislocation density increases as strain increases. Higher number of dislocations leads to increased dynamic recovery and recrystallization and as a result, smaller grains are constituted [28, 29].

In addition to the effect of vibration during FSP on grain size, it seems that it also plays an important role on particle distribution. In Fig. 5, light optical microscopy figures from cross section of processed specimens and in Fig. 6, SEM figures relating to the distribution of second-phase particles as well as Si map analysis by SEM/WDX (wavelength dispersive X-ray) for both FS and FSV processed specimens are observed. In the absence of vibration, SiC particles are not distributed properly and agglomeration of particles occurs largely (Figs. 5a and 6a). For FSV processed specimen, less agglomeration of particles is observed (Figs. 5b and 6b). This can be related to the effect of vibration during FSP which enhances the stir action and correspondingly leads to more homogenous distribution of particles and less agglomeration.

Stress-strain curves of FS and FSV processed specimens as well as base material are seen in Fig. 7. It is observed that ultimate tensile strength of FS and FSV processed specimens are higher than base material; although, their ductility is lower.

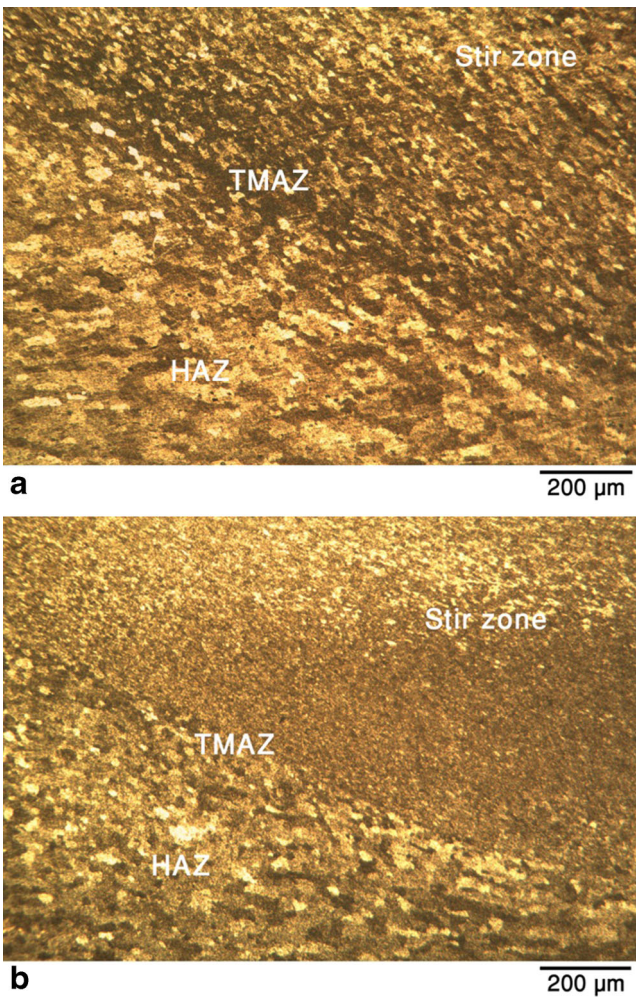

Fig. 4 Processed zones microstructures of **a** FS and **b** FSV processed specimens

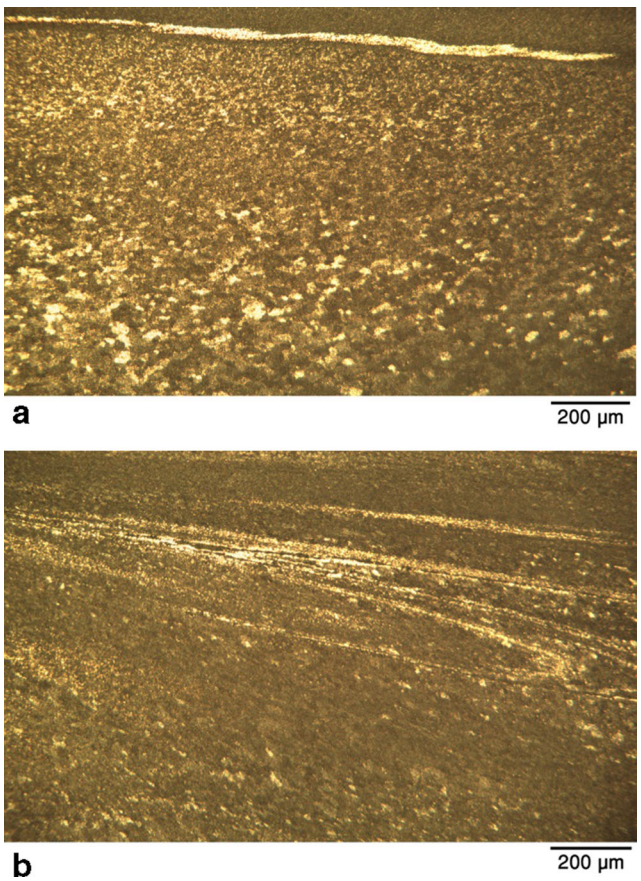

Fig. 5 SiC nanoparticles distribution for **a** FS and **b** FSV processed specimens

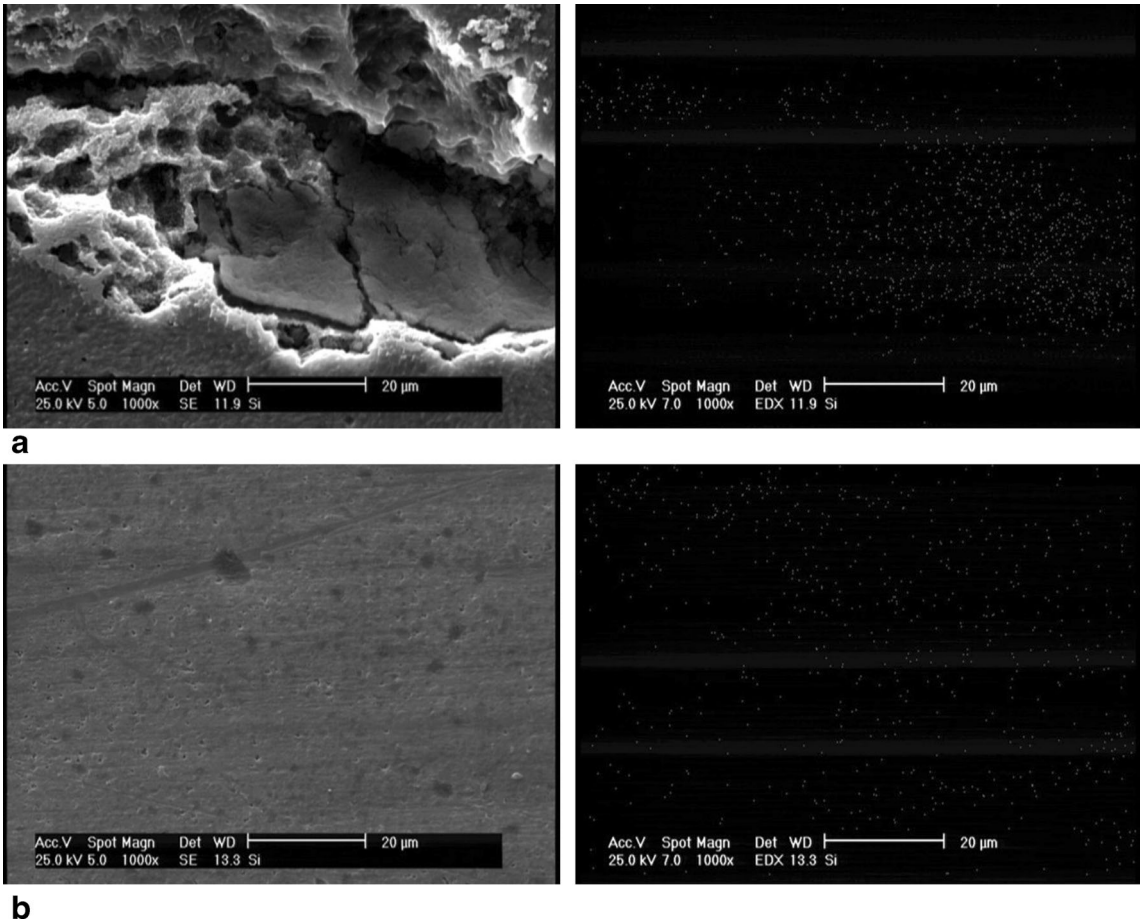

Fig. 6 Particle distribution for **a** FS and **b** FSV processed specimens

Higher strength of processed specimens can be related mainly to presence of second-phase particles in metal matrix which enhance the strength.

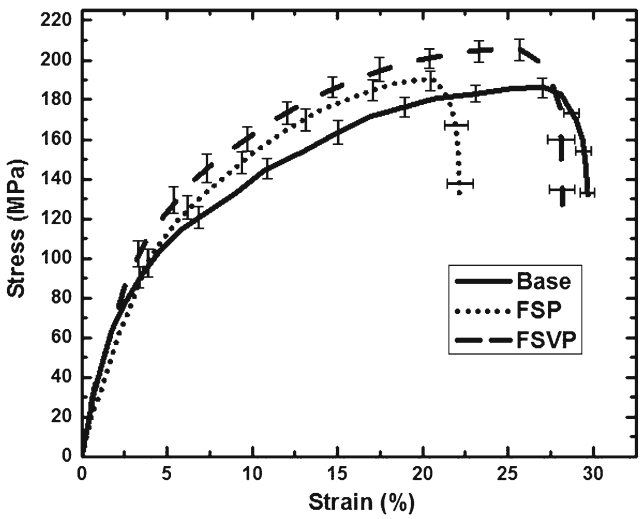

Fig. 7 Stress-strain curves of FS and FSV processed specimens as well as base material

It is also observed in Fig. 7 that strength and ductility of the FSV processed specimens are higher than those of the FS processed specimens. It was observed in Figs. 4 and 5 that the stir zone grain size for the FSV processed specimens was lower than that for FS processed specimens and second-phase particles had more homogenous distribution in the former specimen with regard to the latter one.

Grain boundaries and second-phase particles both can increase the strength and they numerate as two strengthening mechanisms [30, 31]. According to Hall-Petch equation ($\sigma = \sigma_i + kd^{-\frac{1}{2}}$) [32], strength increases as grain size (d) decreases. As grain size decreases, volume fraction of grain boundaries increases and correspondingly the increase to dislocations movement enhances and the strength levels up. Second-phase particles distributed in a ductile matrix are also a common source of alloy strengthening [33]. The degree of strengthening resulting from second-phase particles depends on several factors including the shape, the volume fraction, the average particle diameter, and the interparticle spacing of particles. These factors are all interrelated, so that the change of one factor changes the others [34]. For a given volume fraction of second-phase

particles, the average distance between particles decreases as the particle size decreases. Based on Orowan theory [35], strengthening made by second-phase particles can be presented by the following equation:

$$\Delta\sigma = \frac{\alpha GB}{\lambda}\ln\left(\frac{r}{b}\right)$$

which

α constant
G shear modulus
b bergurs vector
r radius of spherical particles

λ: interparticle spacing and a simple expression for it is $\lambda = \frac{4(1-f)r}{3f}$

where f is the volume fraction of spherical particles of radius r. So, λ decreases and $\Delta\sigma$ increases as r decreases.

For FSV processed specimens, due to presence of vibration, the stir zone grain size (d) is lower than that for FSP processed specimen (Fig. 4) and second-phase particles have more homogenous distribution and are less agglomerated (lower r) (Figs. 5 and 6). In this regard, more strength of FSV processed specimen with regard to FS processed specimen is rational.

Figure 7 also shows that ductility of FSV processed specimens is higher than that for FS processed specimens. This can also be related to lower grain size and more homogenous distribution of second-phase particles in the former specimen with respect to the latter one. Fracture surfaces of both specimens are presented in Fig. 8. Both samples show a dimpled fracture surface which is characteristic of ductile metal fracture surface [36]; although, more dimples are observed for FSV processed specimen.

It has been known that voids initiate and grow during forming of ductile metals and these voids coalesce to form

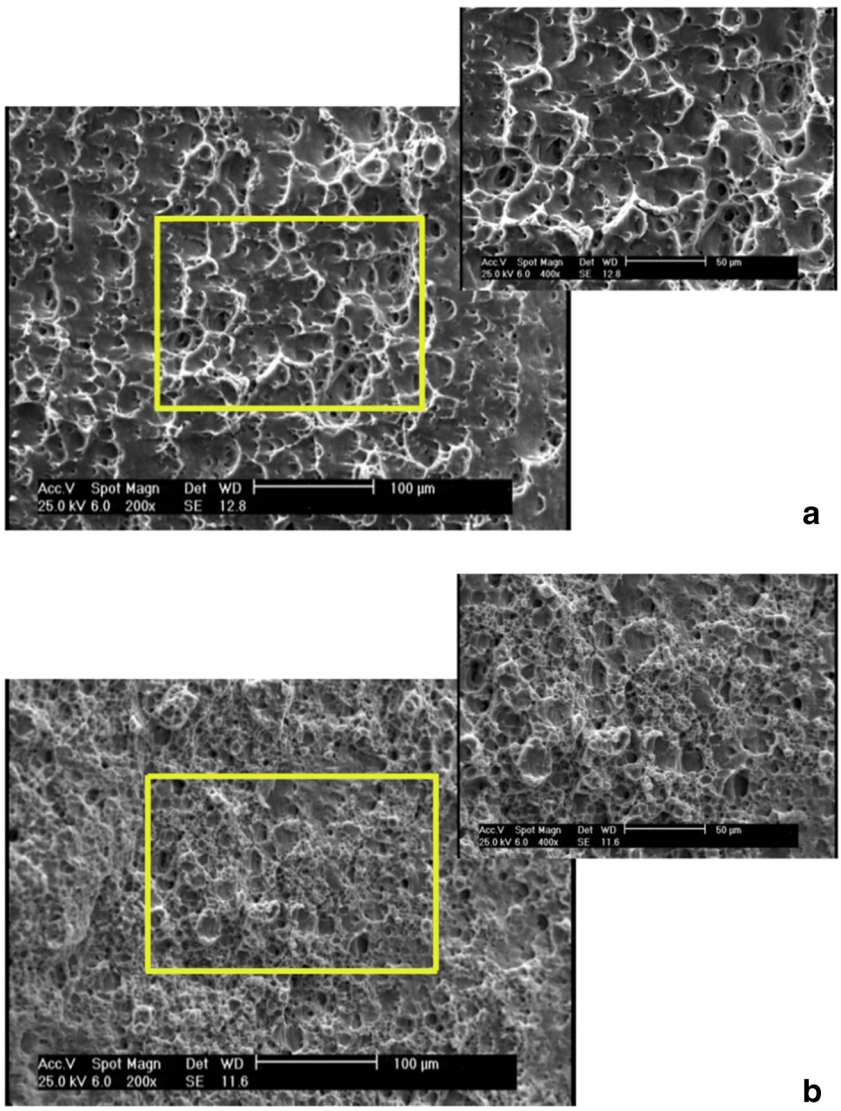

Fig. 8 Fracture surfaces of **a** FS and **b** FSV processed specimens

crack [37]. Coalescence occurs by elongation of the voids and elongation of the bridges of material between the voids [37]. This leads to the formation of a fracture surface consisting of elongated dimples as if it had formed from numerous holes. Voids form at different sites. Particles and precipitations are primary sites for void formation; although, the voids can be generated where special jogs or dislocation locks are forced to move [38]. However, the former voids are larger than the latter ones [37]. Presence of large agglomerated particles in microstructure of FS processed specimen (Fig. 6) results in the formation of large voids and crack growth occurs easily during forming. Figure 8 also shows that voids for the FSV processed specimens are smaller than those for the FS processed specimens. In this regard, lower ductility of FS processed specimens with respect to FSV processed specimens is anticipated.

Hardness analyses revealed that FSV processed specimens had higher hardness in the stir zone (61.52 ± 2 HV) with

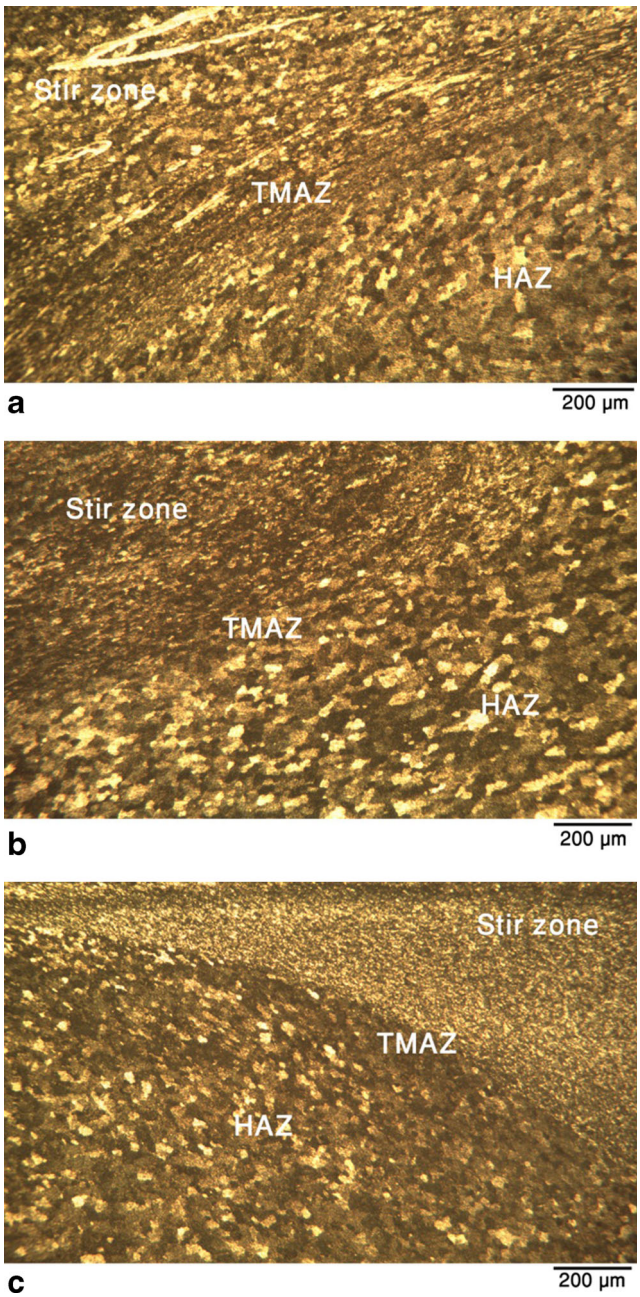

Fig. 9 Processed zones microstructures for FSV processed specimens using different frequencies: **a** 20 Hz, **b** 35 Hz, and **c** 50 Hz

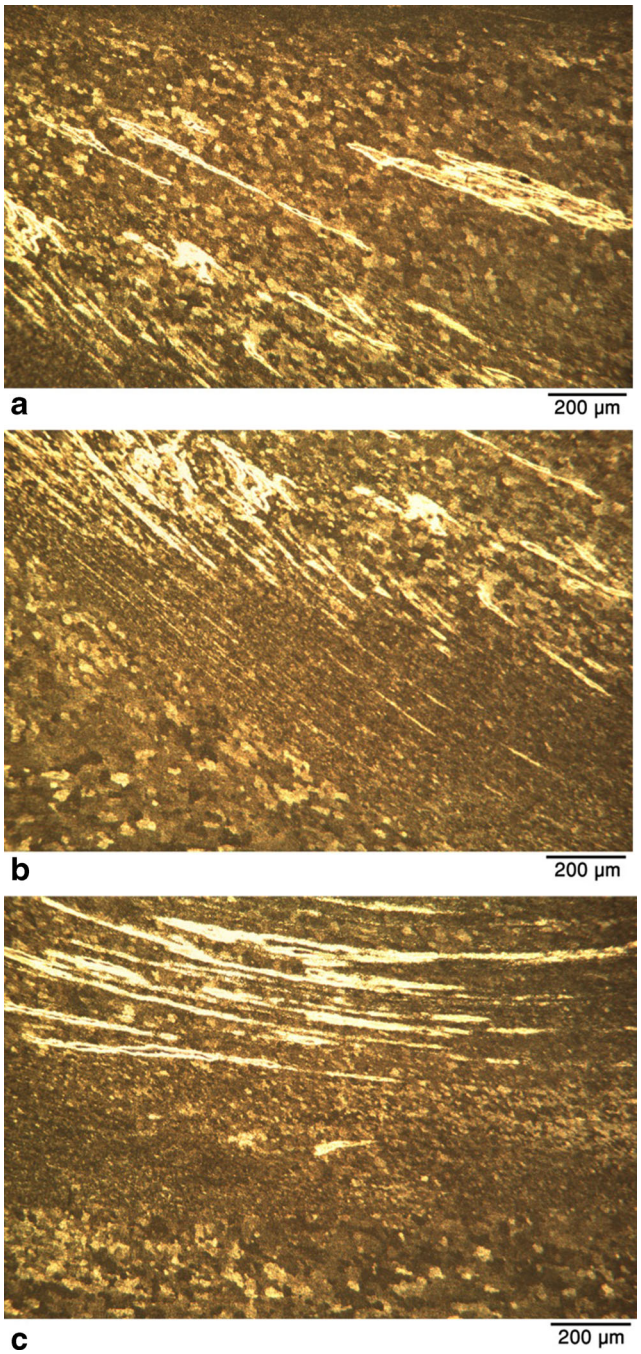

Fig. 10 SiC particle distribution for FSV processed specimens using different frequencies: **a** 20 Hz, **b** 35 Hz, and **c** 50 Hz

respect to FS processed specimens (57.41 ± 2), while hardness for base material was 48.5 ± 1 HV.

3.2 The effect of frequency

Microstructures of FSV processed specimens using different vibration frequencies, namely 20 Hz, 35 Hz and 50 Hz, are presented in Fig. 9. It is observed that as vibration frequency increases, the grain size in the stir zone decreases. As vibration during FSVP increases, due to accompany of vibration movement of substance with transverse and rotation movements of shoulder, material deformation in the stir zone increases, and more strain is applied to metal. Based on refs. [26, 27], dislocations are generated during deformation and their density is proportional to strain value. More strain during FSVP leads to more dislocation density. On the other hand, the main mechanism for grain refinement during FSP is dynamic recrystallization which leads to dislocation rearrangement and

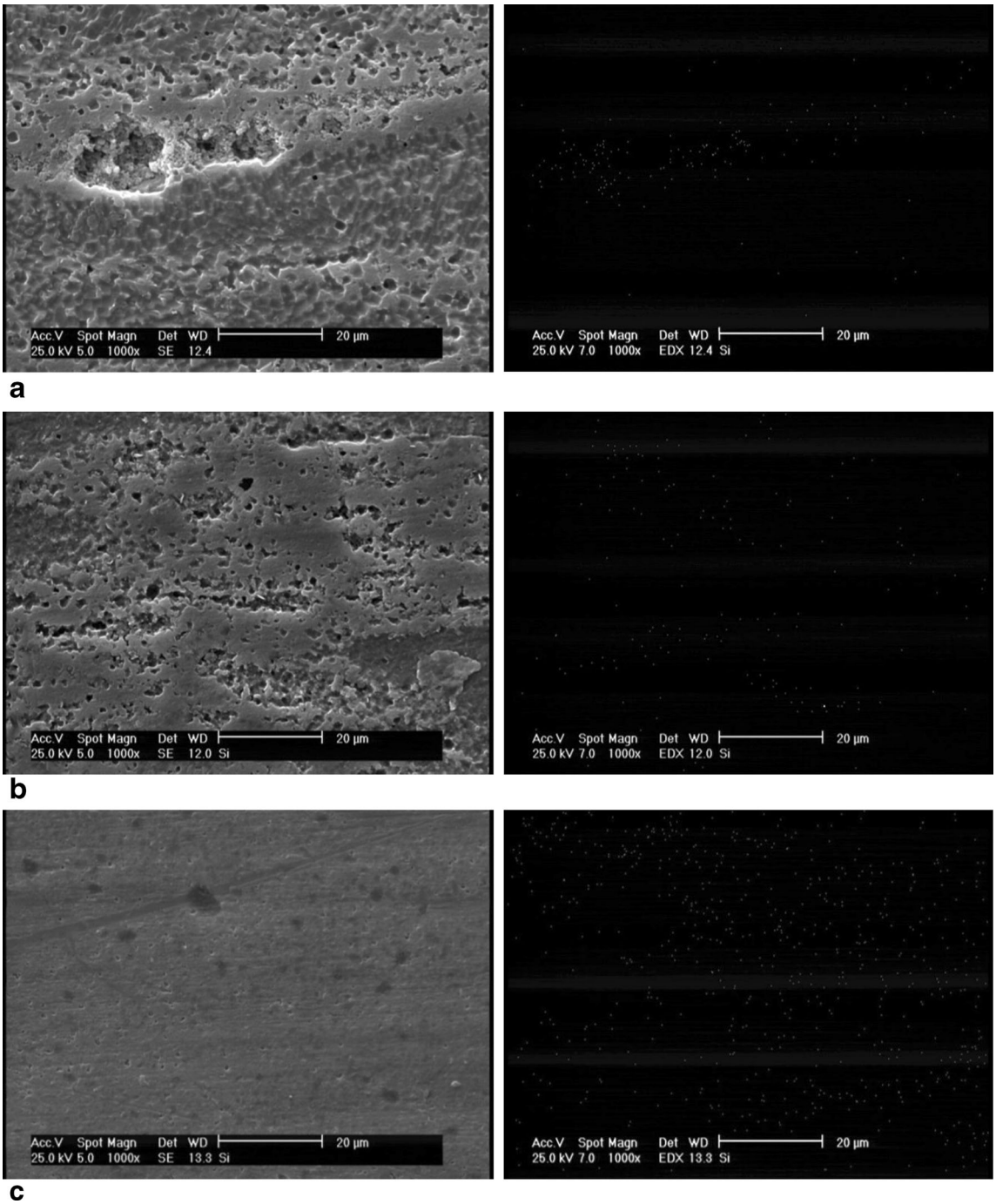

Fig. 11 SiC particle agglomeration and distribution for FSV processed specimens using different frequencies: **a** 20 Hz, **b** 35 Hz, and **c** 50 Hz

constitution of fine grains [24, 25]. More density of dislocations leads to more dynamic recrystallization and correspondingly, finer grains are obtained [28].

Vibration frequency increment role on particle distribution is also important. The effect of vibration frequency on second-phase particles distribution is shown in Figs. 10 and 11. It is seen that distribution homogeneity of particles increases and agglomeration decreases as frequency enhances.

As frequency increases, the material in the stir zone deforms more and the incorporated particles in the matrix are distributed more homogenously. The lower agglomeration of particles, in FSVP, leads to the higher content of smaller agglomerated particles and according to Orowan equation [35], higher strength is anticipated.

Stress-strain curves of FSV processed specimens using different vibration frequencies are shown in Fig. 12. The effect of vibration frequency on the stir zone hardness is also presented in Table 2. UTS and hardness increases can be related to lower grain size (Fig. 9) and smaller agglomerated particles (Fig. 10) due to vibration frequency increase. According to Hall-Petch [32] and Orowan equations [35], these lead to strength and hardness increase.

Ductility increase as a result of vibration frequency increment can also be related to decrease of grain size and size of agglomerated particles in the stir zone. TEM analyses [39, 40] show that grain boundaries increase the dislocation density through the generation of new dislocations called geometrically necessity dislocations (GNDs). GNDs can provide displacement compatibility between grains by accommodating each grain's strain gradient and ductility increases as grain size decreases [40]. Higher ductility of small grains can also be assigned to higher resistance of these grains to crack propagation [41]. Small grains have a higher resistance to crack propagation due to distribution of strain among more grain boundaries. Small agglomerated particles (for FSV processed specimens) also delay formation of voids, with respect to large ones (for FS processed specimens) which lead to large voids, and correspondingly enhance the ductility. Fracture surfaces of FSV processed specimens using various vibration frequencies are presented in Fig. 13. Based on Fig. 13, the specimen processed with the higher frequency shows a fracture surface full of dimples, while for the specimen processed with the lower frequency, dimples are lower but larger. This can be related to more homogenous distribution and less agglomeration of particles as frequency increases. Particles with large size are primary sites for formation of large voids and cracks which eventually lead to early fracture and low ductility [42].

Table 2 Hardness variations in stir zone of FSV processed specimens using different vibration frequencies

Vibration frequency (Hz)	Stir zone hardness (HV)
20	61.5 ± 2
35	64.1 ± 2
50	66.8 ± 2

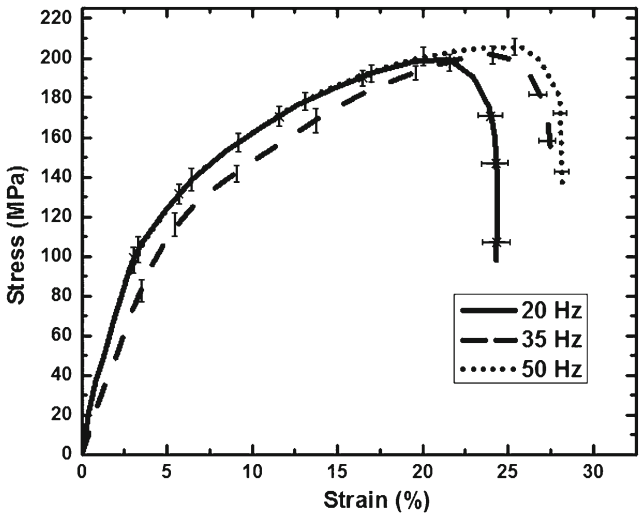

Fig. 12 Stress-strain curves of FSV processed specimens using different frequencies

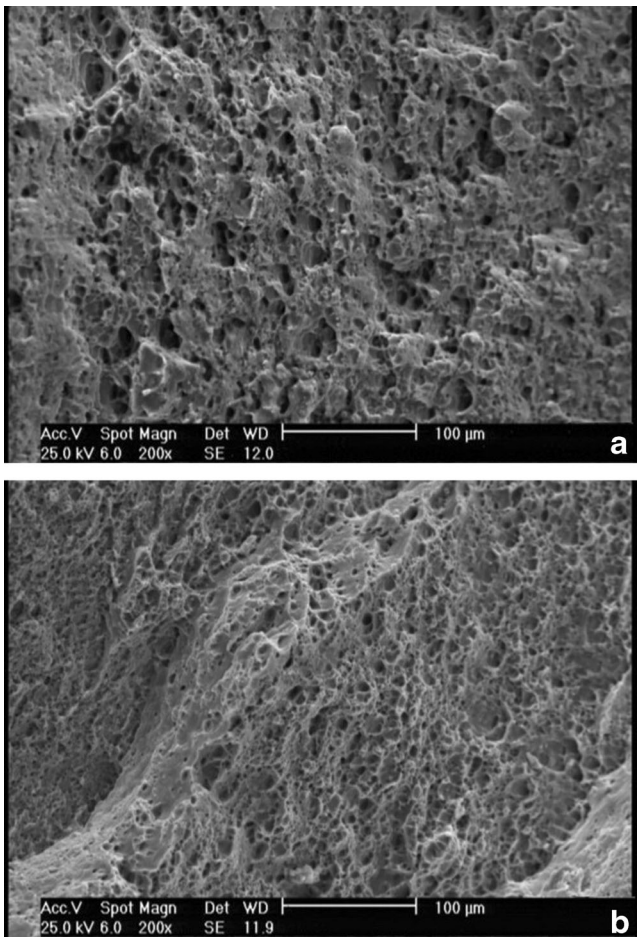

Fig. 13 Fracture surfaces of FSV processed specimens using different frequencies: **a** 20 Hz and **b** 35 Hz

4 Conclusions

In this research, FSVP method was introduced as a new version of FSP. The effect of FSVP on microstructure and mechanical properties of surface composite formed on Al5052 alloy metal surface was investigated. SiC nanoparticles were applied as strengthening particles. Comparison between processed zone microstructures of FS and FSV processed specimens showed that stir zone grain size decreased and particle distribution homogeneity increased as FSVP was applied. The results also indicated that FSV processed specimens had higher strength and ductility with respect to FS processed specimens. It was also observed that strength and ductility of FSV processed specimens increased as vibration frequency increased. It was concluded that presence of vibration during FSP increases the deformation and strain of the soft material in the stir zone and correspondingly, more refined grains are developed in the stir zone, due to enhanced dynamic recrystallization. Additionally, more deformation and movement of material in the stir zone leads to less agglomeration of SiC nanoparticles. Application of FSVP as an "easy to apply" processing method, which enhances the efficiency of FSP, is recommended for industries.

References

1. Mahmoud TS (2013) Surface modification of A390 hypereutectic Al-Si cast alloys using friction stir processing. Surf Coat Technol 228:209–220
2. Chang CI, Du XH, Huang JC (2007) Achieving ultrafine grain size in Mg-Al-Zn alloy by friction stir processing. Scr Mater 57:209–212
3. Kumar N, Mishra RS, Huskamp CS, Sankaran KK (2011) Microstructure and mechanical behavior of friction stir processed ultrafine grained Al-Mg-Sc alloy. Mater Sci Eng A 528:5883–5887
4. Arora KS, Pandy S, Schaper M, Kumar R (2010) Microstructure evolution during friction stir welding of aluminum ally AA2219. J Mater Sci Technol 26:747–753
5. Fu R, Xu H, Luan G, Dong C, Zhang F, Li G (2012) Top surface microstructure of friction stir welded AA2524-T3 aluminum alloy joints. Mater Charact 65:48–54
6. Hannard F, Castin S, Maire E, Mokso R, Pardoen T, Simar A (2017) Ductilization of aluminum alloy 6056 by friction stir processing. Acta Mater 130:121–136
7. Leal RM, Galvao I, Loureiro A, Rodrigues DM (2015) Effect of friction stir processing parameters on the microstructural and electrical properties of copper. Int J Adv Manuf Technol 80:1655–1663
8. Yuvaraj N, Aravindan S, Vipin S (2015) Fabrication of Al5083/B4C surface composite by friction stir processing and its tribological characterization. J Mater Res Technol 4:398–410
9. Abbasi M, Bagheri B, Dadaei M, Omidvar H, Rezaei M. The effect of FSP on mechanical, tribological and corrosion behavior of composite layer developed on magnesium AZ91 alloy surface, Vol 77, 2015, pp. 2051–2058
10. Thankachan T, Prakash KS, Kavimani V (2018) Investigations on the effect of friction stir processing on Cu-BN surface composites. J Mater Manuf Process 33:299–307. https://doi.org/10.1080/10426914.2017.1291952
11. Hussain G, Hashemi R, Hashemi H, Al-Ghamedi KA (2016) An experimental study on multi-pass friction stir processing of Al/TiN composite: some microstructural, mechanical, and wear characteristics. Int J Adv Manuf Technol 84:533–546
12. Zhang Q, Xiao BL, Wang WC, Ma ZY (2012) Relative mechanism and mechanical properties of in situ composites fabricated from an Al-TiO2 system by friction stir processing. Acta Mater 60:7090–7103
13. Ghanbari D, Kasiri Asgarani M, Amini K (2015) Investigating the effect of passes number on microstructural and mechanical properties of the Al2024/SiC composite produced by friction stir processing. Mechanica 6:430–436
14. Ghanbari D, Kasiri Asgarani M, Amini K, Gharavi F (2017) Influence of heat treatment on mechanical properties and microstructure of the Al2024/SiC composite produced by multi-pass friction processing. Measurement 104:151–158
15. Shafiei-Zarghani A, Kashani-Bozorg SF, Zarei-Hanzaki A (2009) Microstructures and mechanical properties of Al/Al2O3 surface nano-composite layer produced by friction stir processing. Mater Sci Eng A 200:84–91
16. Ahmadifard S, Shahin N, Kazemi S, Heidarpour A, Shirazi A (2016) Fabrication of A5083/SiC surface composite by friction stir processing and its characteristics. J Sci Technol Compos 2:31–36
17. Khodabakhshi F, Arab SM, Svec P, Gerlich AP (2017) Fabrication of a new Al-Mg/grapheme nanocomposite by multi-pass friction-stir processing: dispersion, microstructure, stability and strengthening. Mater Charact 132:92–107
18. Dadaei M, Omidvar H, Bagheri B, Jahazi M, Abbasi M (2014) The effect of SiC/Al2O3 particles used during FSP on mechanical properties of AZ91 magnesium alloy. Int J Mater Res 105:369–374
19. ASTM (2017) E3-11 (2017) Standard guide for preparation of metallographic specimens. ASTM International, West Conshohocken
20. ASTM (2016) E8/E8M-16a, Standard test methods for tension testing of metallic materials. ASTM International, West Conshohocken
21. ASTM (2017) E92-17, Standard test methods for Vickers hardness and Knoop hardness of metallic materials. ASTM International, West Conshohocken
22. Huang Y, Wang Y, Meng X, Wan L, Cao J, Zhou L, Feng J (2017) Dynamic recrystallization and mechanical properties of friction stir processed Mg-Zn-Y-Zr alloys. J Mater Process Technol 249:331–338. https://doi.org/10.1016/j.jmatprotec.2017.06.021
23. Rao AG, Ravi KR, Ramakrishnarao B, Deshmukh VP, Sharma A, Prabhu N, Kashyap BP (2013) Recrystallization phenomena during friction stir processing of hypereutectic aluminum-silicon alloy. Metall Mater Trans A 44:1519–1529
24. Su JQ, Nelson TW, Sterling CJ (2006) Grain refinement of aluminum alloys by friction stir processing. Philos Mag 86:1–24
25. Behnagh RA, Shen N, Abdollahi M, Ding H (2016) Ultrafine-grained surface layer formation of aluminum alloy 5083 by friction stir processing. Procedia CIRP 45:243–246
26. Hull D, Bacon DJ (2011) Introduction to dislocations, Elsevier Ltd, 5th ed. USA
27. Barooni O, Abbasi M, Givi M, Bagheri B (2017) New method to improve the microstructure and mechanical properties of joint obtained using FSW. Int J Adv Manuf Technol 93:4371–4378
28. Rahmi M, Abbasi M (2017) Friction stir vibration welding process: modified version of friction stir welding process. Int J Adv Manuf Technol 90:141–151
29. Fouladi S, Ghasemi AH, Abbasi M, Abedini M, Khorasani AM, Gibson I (2017) The effect of vibration during friction stir welding

on corrosion behavior, mechanical properties, and machining characteristics of stir zone. Metals 7:421–435
30. Callister WD (2007) Materials science and engineering: an introduction. Wiley, USA
31. Naderi M, Abbasi M, Saeed-Akbari A (2013) Enhanced mechanical properties of a hot-stamped advanced high-strength steel via tempering treatment. Metall Mater Trans A 44: 1852–1861
32. Du D, Fu R, Li Y, Jing L, Wang J, Ren Y, Yang K (2015) Modification of the Hall–Petch equation for friction-stir-processing microstructures of high-nitrogen steel. Mater Sci Eng A 640:190–194
33. Jeon CH, et al. (2014) Material properties of graphene/aluminum metal matrix composites fabricated by friction stir processing. Int J Precis Eng Manuf 15:1235–1239
34. Dieter GE (1988) Mechanical metallurgy. McGraw-Hill Book Company, Singapore
35. Kulkarni AJ, Krishnamurthy K, Deshmukh SP, Mishra RS (2004) Effect of particle size distribution on strength of precipitation-hardened alloys. J Mater Res 19:2765–2773
36. Abbasi M, Shafaat MA, Ketabchi M, Haghshenas D, Abbasi M (2012) Application of the GTN model to predict the forming limit diagram of IF steel. J Mech Sci Technol 26:345–352
37. V. Uthaisangsuk, Microstructure based formability modeling of multiphase steels, Ph. D. Thesis, IEHK, RWTH- Aachen, 2009
38. Hertzberg RW (1996) Deformation and fracture mechanics of engineering materials, 4th edn. John Wiley & Sons Inc, USA, pp 135–139
39. Schempp P, Cross CE, Hacker R, Pittner A, Rethmeier M (2013) Influence of grain size on mechanical properties of aluminum GTA weld metal. Weld World 57:293–304
40. Hansen N (1977) The effect of grain size and strain on the tensile flow stress of aluminum at room temperature. Acta Metall 25:863–869
41. Spittle JA, Cushway AA (1983) Influence of superheat and grain structure on hot-tearing susceptibilities of Al-Cu alloy castings. Metals Technol 10:6–13
42. Yu H, Tieu K, Lu C, Lou Y, Liu X, Godbole A, Kong C (2014) Tensile fracture of ultrafine grained aluminum 6061 sheets by asymmetric cryorolling for microforming. Int J Damage Mech 23: 1077–1095